



Toward plasmonics-enabled spatiotemporal activity patterns in three-dimensional culture models

Somin Eunice Lee, A Paul Alivisatos & Mina J Bissell

To cite this article: Somin Eunice Lee, A Paul Alivisatos & Mina J Bissell (2013) Toward plasmonics-enabled spatiotemporal activity patterns in three-dimensional culture models, Systems Biomedicine, 1:1, 12-19, DOI: [10.4161/sysb.22834](https://doi.org/10.4161/sysb.22834)

To link to this article: <https://doi.org/10.4161/sysb.22834>



Copyright © 2013 Landes Bioscience



Published online: 01 Jan 2013.



Submit your article to this journal [↗](#)



Article views: 604



View related articles [↗](#)



Citing articles: 2 View citing articles [↗](#)

Toward plasmonics-enabled spatiotemporal activity patterns in three-dimensional culture models

Somin Eunice Lee,^{1,2,3} A Paul Alivisatos^{2,3} and Mina J Bissell^{1,*}

¹Life Sciences Division; Lawrence Berkeley National Laboratory; Berkeley, CA USA; ²Material Science Division; Lawrence Berkeley National Laboratory; Berkeley, CA USA; ³Department of Chemistry; University of California at Berkeley; Berkeley, CA USA

Keywords: gold nanocrystal, gold nanoparticle, plasmon ruler, plasmon coupling, protease activity, tissue morphogenesis, branching morphogenesis, migration, metastasis

Spatiotemporal activity patterns of proteases such as matrix metalloproteinases and cysteine proteases in organs have the potential to provide insight into how organized structural patterns arise during tissue morphogenesis and may suggest therapeutic strategies to repair diseased tissues. Toward imaging spatiotemporal activity patterns, recently increased emphasis has been placed on imaging activity patterns in three-dimensional culture models that resemble tissues *in vivo*. Here, we briefly review key methods, based on fluorogenic modifications either to the extracellular matrix or to the protease of interest, that have allowed for qualitative imaging of activity patterns in three-dimensional culture models. We highlight emerging plasmonic methods that address significant improvements in spatial and temporal resolution and have the potential to enable quantitative measurement of spatiotemporal activity patterns with single-molecule sensitivity.

Introduction

During tissue morphogenesis, individual cells organize into complex yet highly organized patterns to form multi-cellular tissues of distinct shapes and structure (Fig. 1). Yet little is understood about exactly how these organized structural patterns arise during the formation process. For example, in branching morphogenesis of many branched tubular networks, cells first develop or organize into a hollow epithelial tubule or sac. Subgroups of cells are then directed to form new branches. Through a reiterative process of branch initiation and invasion, a tree-like structure is formed as seen in many organs such as kidneys, salivary glands and mammary glands.^{1–5} How these epithelial cells are spatially and temporally coordinated to produce highly organized branching patterns is not yet well understood. It is postulated that branching morphogenesis arises, in part, as a result of localized remodeling and degradation of the extracellular matrix by proteases, such as matrix metalloproteinases^{6,7} and cysteine proteases.⁸ In many cases, proteases are initially maintained in an

inactive conformation. Upon modulation by the microenvironment via external environmental stimuli of chemical nature (e.g., growth factors, cytokines, hormones) and physical nature (e.g., tensile stress, compressive stress), proteases are activated to presumably remodel and degrade the extracellular matrix, allowing cells to invade into the stroma.^{6,9} Proteases also interact with each other in complex proteolytic networks^{10,11} and liberate cytokines and growth factors embedded within the extracellular matrix.¹² Clearly, then, proteases must be spatially and temporally organized in a developing tissue. Therefore, knowing the spatial context (i.e., the precise location at which an active protease exercises its biochemical function) and temporal context (i.e., the precise time a protease exercises its biochemical catalytic function) should provide insight into these mechanisms orchestrating branching morphogenesis, and may suggest therapeutic strategies to repair diseased tissues.

To illustrate the importance of spatial and temporal patterns, suppose that a forming tissue is analogous to a sensor (Fig. 1A). A sensor measures external input stimuli and converts these signals into an output response. The function of the sensor depends on the stimuli-response relationship. The same is true of a forming tissue (Fig. 1B): it processes environmental input stimuli into an output response of activated proteases that in part facilitates the collective rearrangement of cells into an organized tissue structure. In this context, the process of branching morphogenesis can be thought of as a function that depends on the environmental input stimuli with the output response being that of activated proteases. Taking into account that tissues within the organs are three-dimensional, tissues could be viewed as three-dimensional arrays of sensors. At no location in the tissue is the composition of cells and extracellular matrix constant. It is reasonable to assume that environmental stimuli would also vary spatially and temporally across the three-dimensional structure. Thus, the output response of activated proteases also would not be constant, but would vary spatially and temporally across the structure as the tissue develops. Understanding the importance of these dynamics requires quantitative measurement of spatiotemporal activity patterns (Fig. 3), which cannot be acquired using conventional ensemble techniques, such as electrophoretic zymographies, western blots and other biochemical techniques.

*Correspondence to: Mina J Bissell; Email: mjbissell@lbl.gov
Submitted: 09/26/12; Accepted: 10/16/12
<http://dx.doi.org/10.4161/sysb.22834>

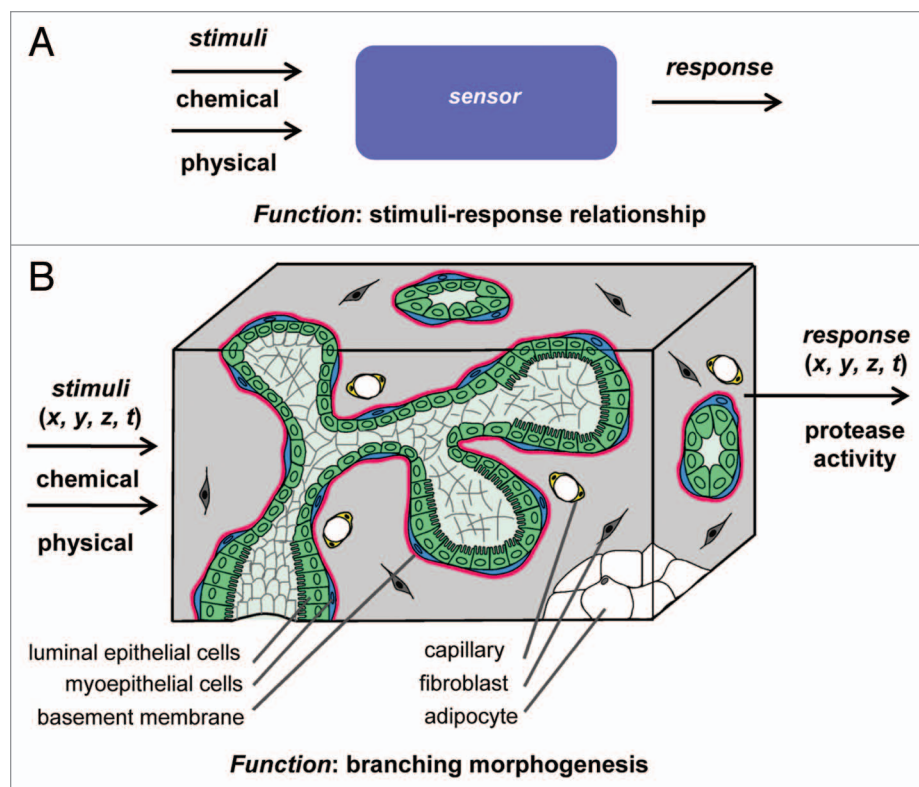


Figure 1. Spatiotemporal stimuli-response for a three-dimensional tissue. (A) Tissues could be viewed as analogous sensors. A sensor measures external input stimuli and converts these signals into an output response, where the sensor function depends on this stimuli-response relationship. (B) Analogous to a three-dimensional array of sensors, a three-dimensional tissue spatiotemporally processes chemical and physical environmental input stimuli (e.g., growth factors, cytokines, hormones, tensile stress, and compressive stress). The process of epithelial branching morphogenesis within a tissue then is a function that depends on the environmental input stimuli at (x, y, z, t) , leading to an output response of activated proteases at (x, y, z, t) that, in part, gives rise to an organized branched structure within the tissue. The branched structure depicted here consists of a hollow lumen surrounded by layers of luminal epithelial cells, myoepithelial cells and a basement membrane. This structure is then surrounded by a stroma containing capillaries, fibroblasts, adipocytes, among others (adapted with permission from ref. 2).

Toward the goal of quantitative spatiotemporal activity patterns, recently increased emphasis has been placed on imaging activity patterns in three-dimensional culture models¹³⁻¹⁸ that resemble *in vivo* tissues.^{2,6,19-21} Qualitative activity patterns, displaying localized activity in acinar structures¹⁸ and in migratory cells²² of three-dimensional culture models, have been reported. Improvements in spatial and temporal resolution should allow qualitative activity patterns to become more quantitative. Plasmonic methods address significant improvements in both spatial and temporal resolution,²³⁻²⁸ and have the potential to enable quantitative measurement of spatiotemporal activity patterns. These patterns in three-dimensional culture models combined with *in vivo* models are expected to lead to improved quantitative descriptions of tissue morphogenesis and possibly also advance therapeutic approaches to pinpoint when and where intervention can be effected to repair diseased or defective tissues.

Activity Patterns

Imaging activity patterns in three-dimensional culture models that recapitulate tissue structures *in vivo* presents a tractable starting point to begin understanding how organized spatial patterns arise during tissue morphogenesis. A tissue-like structure can be produced when epithelial cells are grown in a three-dimensional extracellular matrix.²⁰ To image activity patterns in three-dimensional culture models, several methods, based on fluorogenic modifications either to the extracellular matrix or to the protease-of-interest, have been developed.¹³⁻¹⁸ In many cases, improvements in spatial resolution were reported to allow precise visualization of localization of activity patterns.

Such activity patterns, based on incorporation of protease-cleavable fluorogenic protein substrates into the extracellular matrix, have been the most commonly reported.^{13,15-17} Cleavable full-length proteins, such as collagen I or collagen IV, are designed to be recognized and cleaved by a family of proteases. These proteins are heavily modified with fluorophores in order for the fluorophores to be in close proximity so that they would be able to self-quench. These fluorogenic protein substrates are then simply combined with extracellular matrix in three-dimensional culture models (Fig. 2A and B). When the fluorogenic protein substrates are degraded by proteases, fluorophores become separated and no longer self-quench, restoring fluorescence. Thus, fluorescence reports sites of activity. For example, using fluorogenic collagen I protein (DQTM collagen I) in three-dimensional human fibrosarcoma culture models,^{16,17} proteinase activity patterns were imaged during cell migration (Fig. 2A). The authors argued that these activity patterns demonstrate focalized cleavage of collagen fibers during cell migration and postulated an alternative mechanism for tumor cell migration,¹⁶ although this alternative hypothesis is still disputed.¹⁴ Whereas this visualization method is perhaps the simplest, activity patterns acquired by this method are at best qualitative. Precise localization of activity is challenging because post-degradation, the fluorophores are able to freely diffuse away from the site of activity, limiting spatial resolution.

Spatial resolution of activity patterns can be significantly improved by covalently anchoring a protease-cleavable fluorogenic peptide substrate to the extracellular matrix.²² Cleavable peptide substrates have been designed to be recognized and cleaved by a family of proteases^{22,29-31} or by a specific protease.^{32,33} In this visualization method, a cleavable peptide substrate is modified

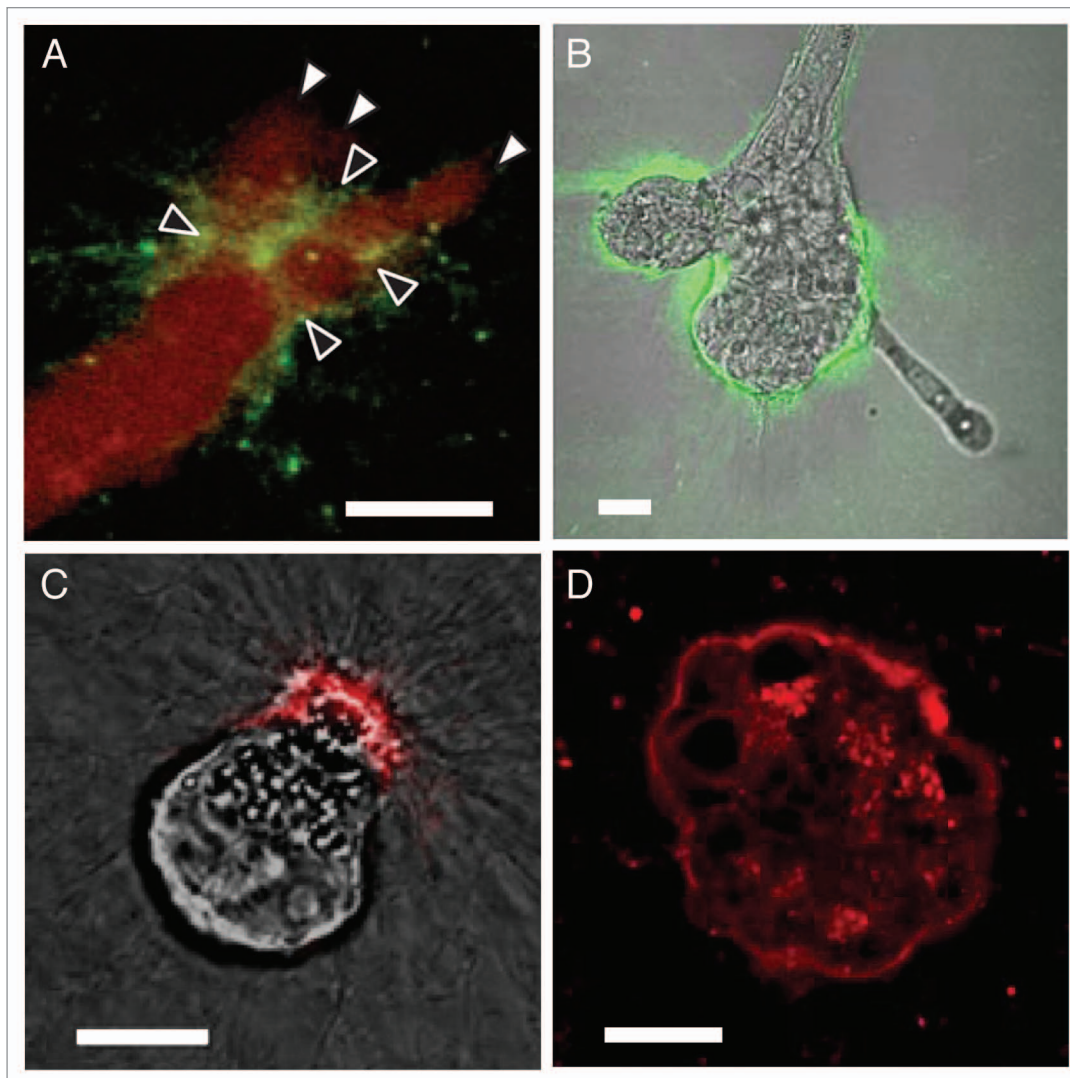


Figure 2. Activity patterns of proteases in three-dimensional culture models. (A) Proteinase activity by cleavable fluorogenic collagen I protein (DQ™ collagen I) in three-dimensional human fibrosarcoma culture model (adapted from ref. 16). (B) Proteinase activity by cleavable fluorogenic collagen IV protein (DQ™ collagen IV) in three-dimensional human breast carcinoma culture model (adapted from ref. 15). (C) Membrane-bound matrix metalloproteinase activity by cleavable fluorogenic peptide substrates in three-dimensional human prostatic carcinoma culture model (adapted from ref. 22). (D) Intracellular cysteine cathepsin protease activity by fluorogenic peptide scaffolds in three-dimensional human mammary epithelial culture model (adapted from ref. 18). Scale bars: 10 μm .

on each end with self-quenching fluorophores. The fluorophores are conjugated to a peptidyl backbone that anchors via chemical cross-linking to the extracellular matrix of three-dimensional culture models. When the fluorogenic peptide substrate is cleaved by a protease, the fluorophores separate and become fluorescent such that one of the fluorophores remains immobilized while the other fluorophore diffuses away. Since one of the fluorophores is anchored to the extracellular matrix and therefore remains at the site of activity, precise spatial localization can be achieved. Activity patterns in three-dimensional human prostatic carcinoma culture models revealed that membrane-bound matrix metalloproteinases were localized specifically at the polarized leading edge of migrating cells (Fig. 2C).²² Using an alternative anchoring strategy, improved spatial resolution has also been shown by anchoring a cleavable peptide substrate, modified on

each end with fluorescent proteins displaying fluorescence resonance energy transfer, to a membrane receptor adjacent to the membrane-bound matrix metalloproteinase. The activity of this protease was imaged via fluorescence resonance energy transfer with high spatial resolution.³⁴

Another strategy to improve spatial resolution of activity patterns is to directly attach a fluorogenic peptide scaffold to an active protease.^{18,35-41} Fluorogenic peptide scaffolds have been designed for covalent attachment to both intracellular^{18,35,39,40} and extracellular^{37,41} active proteases. The fluorogenic peptide scaffold covalently binds to a catalytic residue in the protease's active site. Since the fluorogenic peptide remains covalently bound to the active site, spatial localization can be achieved. The inactive form of the protease remains unmodified as its active site is presumably not exposed. Thus, this visualization method allows active

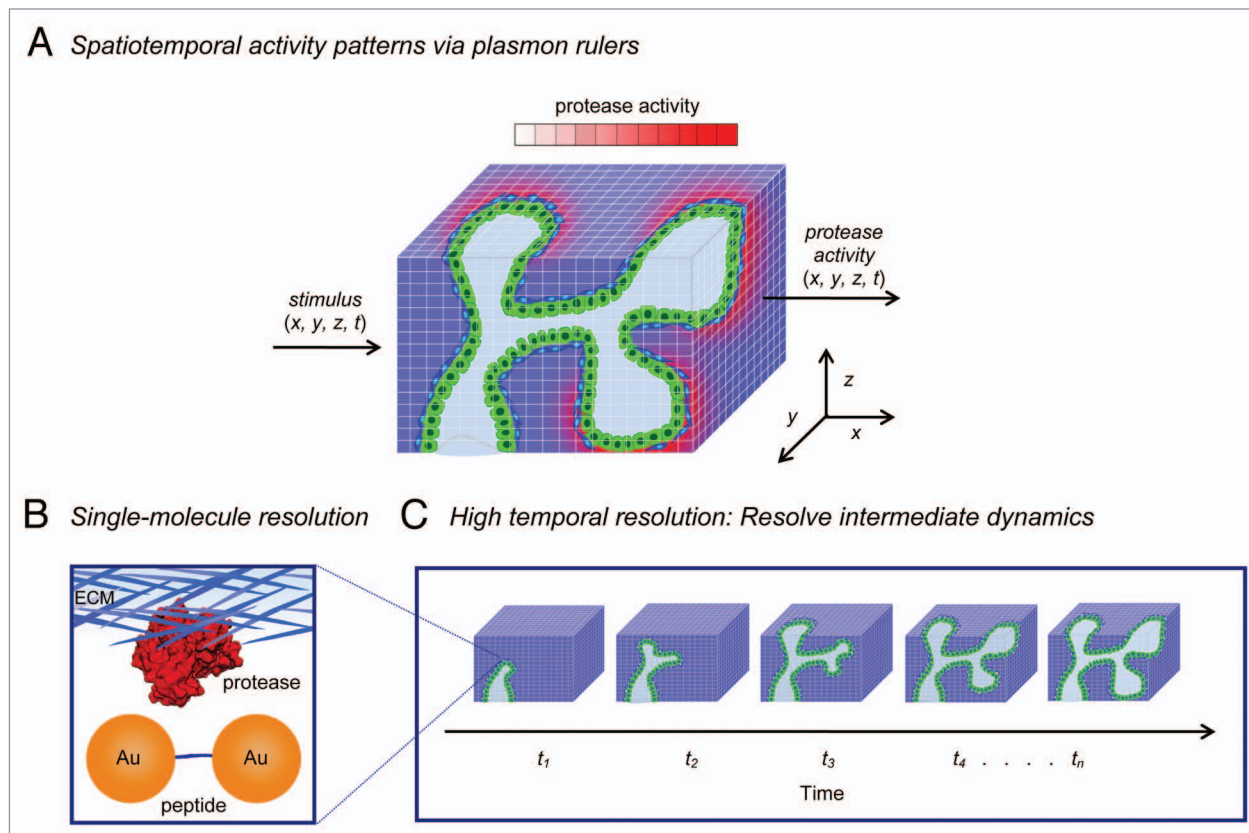


Figure 3. Concept of spatiotemporal activity patterns via plasmon rulers. **(A)** Spatiotemporal activity pattern of proteases as a function of environmental input stimulus (x, y, z, t) . Plasmon rulers address significant improvements in spatial and temporal resolution and should enable quantitative measurement of spatiotemporal activity patterns. **(B)** Single-molecule resolution: image single cleaving or binding event with single-molecule resolution using plasmon rulers consisting of peptide-linked gold nanocrystals in the extracellular matrix (ECM). **(C)** High temporal resolution: image intermediate dynamics in activity patterns since plasmon rulers can be continuously imaged in real-time with potentially unlimited number of acquisitions in an imaging time period, resulting in high temporal resolution over the course of the imaging time period.

and inactive forms of proteases to be distinguished. For example, active cysteine cathepsin proteases were modified using a fluorogenic peptide acyloxymethyl ketone, consisting of a fluorophore and quenching group attached to an acyloxy leaving group.¹⁸ Initially, the fluorescence was quenched. Covalent binding of the fluorogenic peptide to a catalytic residue in the active site of the protease caused a loss of the quenching group, resulting in fluorescence. Using this technique, activity patterns of intracellular cysteine cathepsin proteases were imaged in three-dimensional human mammary epithelial culture models and showed distinct localization of these proteases in lysosomal compartments in acinar structures (Fig. 2D).¹⁸

These methods present several strategies to improve spatial resolution of activity patterns acquired from three-dimensional culture models. However, to move toward quantitative activity patterns, improved temporal resolution is needed in addition to spatial resolution. The methods mentioned above are all based on modifications with fluorophores and suffer from photobleaching inherent to organic dye-based and protein-based fluorophores. Photobleaching often limits the number of acquisitions possible in the required imaging time period (i.e., days), resulting in low temporal resolution over the course of the imaging time period.

The time-dependent characteristics of photobleaching can also interfere with the interpretation of temporal information in activity patterns. Colloidal quantum dot-based modifications are an improvement;⁴²⁻⁴⁴ however, quantum dots also are susceptible to photobleaching and complex blinking. As a consequence, acquiring quantitative temporal information in activity patterns is currently very difficult, and thus reported activity patterns so far have provided only a qualitative picture of cellular invasion within developing tissues.

Toward Spatiotemporal Activity Patterns via Plasmon Rulers

Spatiotemporal activity patterns, displaying high spatial and temporal resolution, would allow for an improved quantitative description of tissue morphogenesis. There is a clear need for probes that are capable of high spatial and temporal resolution. Plasmon rulers, consisting of coupled gold nanocrystals, have the potential to play an important role as improved probes for measuring quantitative spatiotemporal activity patterns (Fig. 3).

Improved temporal resolution arises inherently from the physical properties of a gold nanocrystal. A gold nanocrystal exhibits a

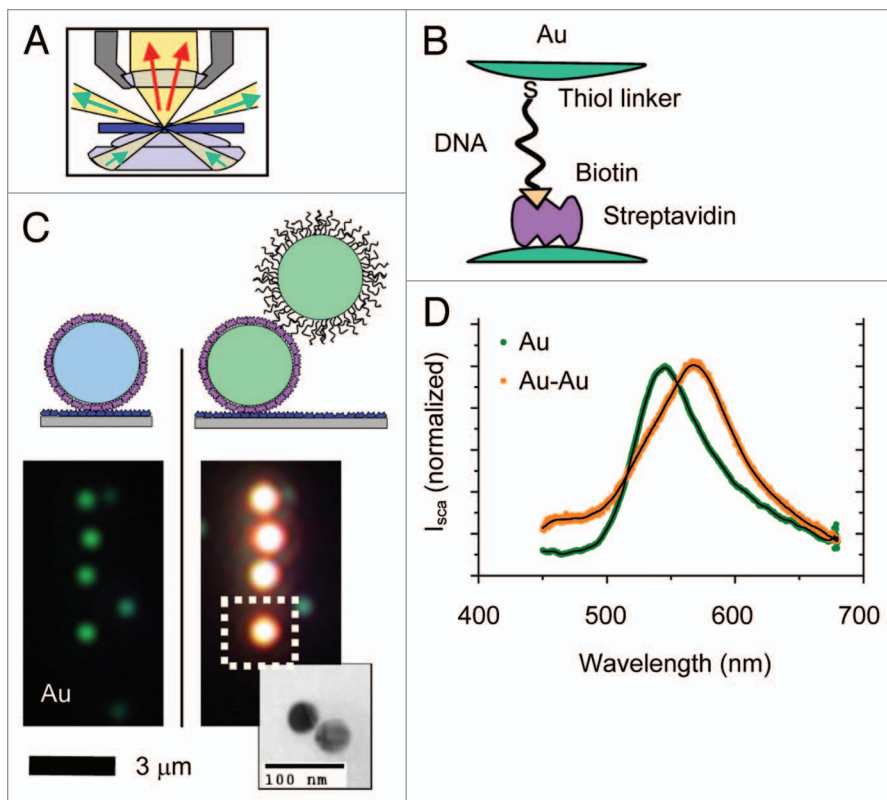


Figure 4. Plasmon rulers. (A) Single gold nanocrystals and coupled gold nanocrystals imaged by illuminating with unpolarized white light and collecting scattered light using a darkfield microscope in transmission mode. (B) Plasmon ruler consists of two gold nanocrystals coupled together using DNA linker. (C) Single gold nanocrystals appear green and coupled gold nanocrystals appear orange in darkfield images. Inset: representative transmission electron microscopy image of coupled gold nanocrystals. (D) Darkfield light scattering spectra from a single gold nanocrystal and coupled gold nanocrystals (adapted with permission from ref. 23).

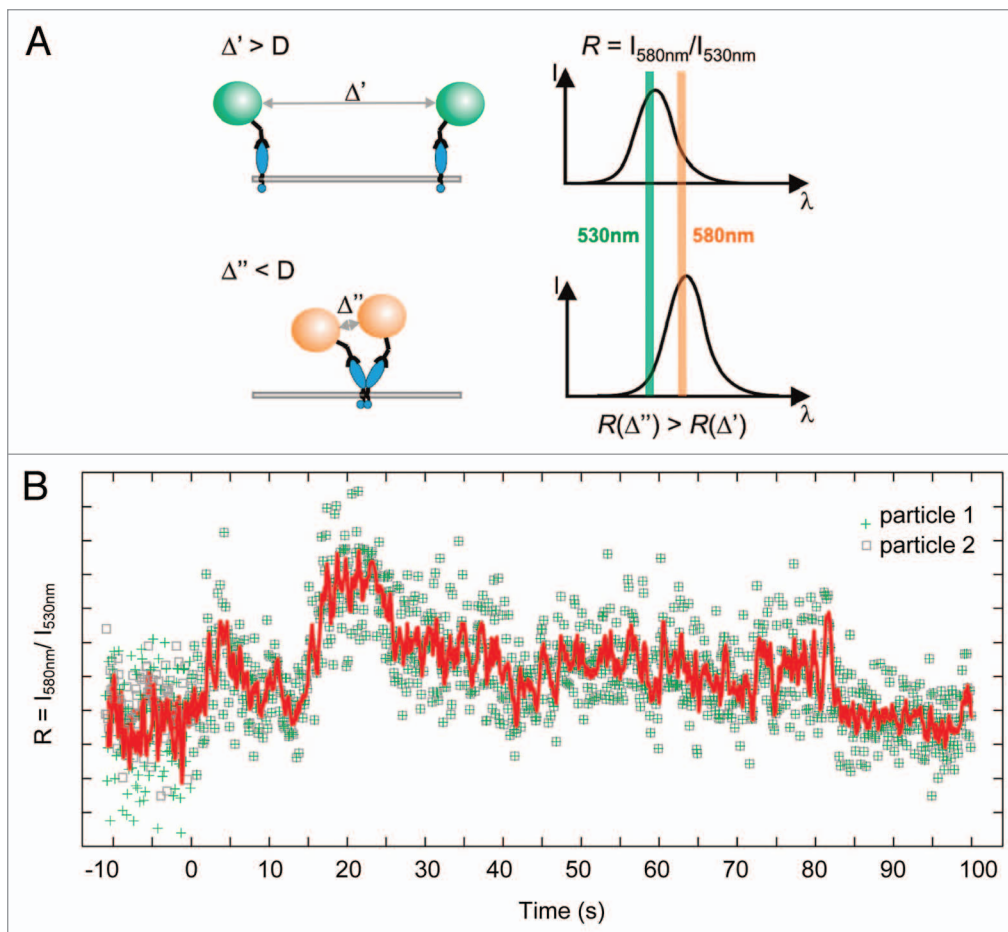


Figure 5. Receptor colocalization visualized at the single-molecule level. (A) Single gold nanocrystals bound to individual surface receptors. Individual receptors visualized at the single-molecule level. Colocalization of individual receptors visualized with subdiffraction resolution by plasmon coupling of the gold nanocrystal labeled separations Δ larger than the particle diameter $D = 40$ nm, no surface plasmon coupling occurs. For interparticle separations $\Delta < D$, surface plasmon coupling occurs due to colocalization of receptors, resulting in an increase in the intensity ratio $R = I_{580\text{nm}}/I_{530\text{nm}}$. (B) Intensity ratio $R = I_{580\text{nm}}/I_{530\text{nm}}$ values for two gold nanocrystal labels diffusing on the surface of a cell as a function of time. The observed increase in R after colocalization, most prominently between time 16.5 s and 25.5 s, indicates that the nanocrystals approach each other close enough for plasmon coupling to occur (adapted from ref. 25).

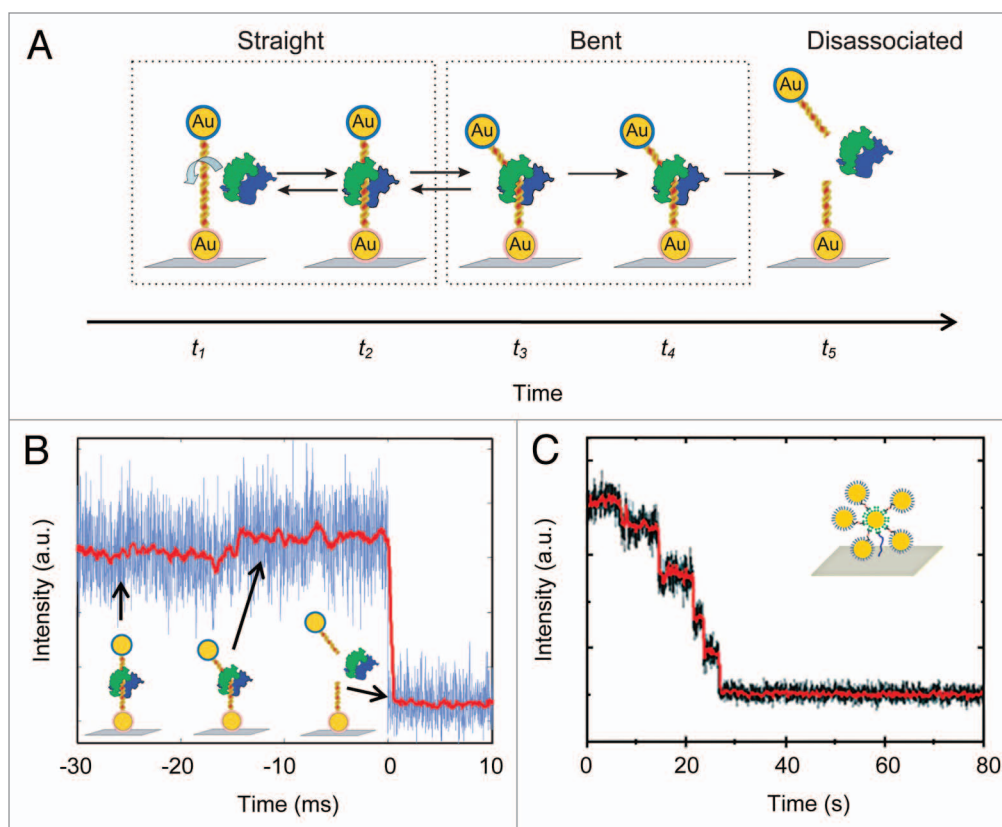


Figure 6. High temporal resolution of plasmon rulers resolves intermediate dynamics. (A) Plasmon ruler consists of a gold nanocrystal dimer linked with DNA containing a single restriction site for a restriction enzyme EcoRV. Intermediate events over time: The enzyme first binds non-specifically, translocates and binds to the target site, bends the DNA at the target site, cuts the DNA, and finally releases the products. (B) Intermediate events monitored by plasmon coupling over time. The bending of the DNA causes the two nanocrystals to become closer, resulting in a decrease in the interparticle distance and therefore an increase in the light scattering intensity. The enzyme then cut the DNA and a decrease in the light scattering intensity is seen (adapted from ref. 24). (C) Peptide cleavage events monitored over time using plasmon ruler consisting of peptide-linked nanocrystals (adapted from ref. 26).

surface plasmon in the presence of an electromagnetic field. A surface plasmon is the collective oscillation of electrons at the interface between two materials, in this case, the metal nanocrystal and the dielectric local environment. The surface plasmon is most prominent at the resonance condition where the wavelength of the electromagnetic field is matched to the resonance wavelength of the nanocrystal, allowing for coupling to occur between the electromagnetic field and the electrons.⁴⁵ The nanocrystal resonance wavelength depends on the shape, size, and local environment of the nanocrystal.⁴⁶ This resonance can result in intense light scattering from the nanocrystal that is constant with respect to time. The light scattering spectrum is time-invariant and can be continuously acquired in real-time in a few milliseconds, resulting in high (ms) temporal resolution over the course of long imaging periods. Potentially as long as hours or even days, the total imaging time is not limited by the properties of the probe nanoparticle.

Improved spatial resolution arises from the physical mechanism of coupled gold nanocrystals. Two gold nanocrystals can be coupled together using a single biomolecule substrate (i.e., cleavable peptide substrate, peptide scaffold), where the substrate length determines the distance between the two nanocrystals. The substrate length is designed so that the distance between the two nanocrystals is less than their diameter. In this configuration,

the surface plasmons of each nanocrystal couple together, resulting in a shift in the resonance wavelength. The strength of this surface plasmon coupling and the resulting wavelength shift is dependent on the distance between the two nanocrystals,^{23,47,48} and can be colorimetrically and spectroscopically observed (Fig. 4C and D). In the event that cleaving or binding occurs to the biomolecule substrate, the distance between the two nanocrystals will change, which is observable in the light scattering spectrum. Since changes in surface plasmon resonance wavelength can be correlated with changes in distance,^{47,48} coupled gold nanocrystals, otherwise referred to as a plasmon ruler, can be used to observe a single cleaving or binding event.^{23,24,26,49-52} High spatial resolution is achievable because of the large scattering cross-section and therefore high intensity of the scattered spectrum, permitting the analysis of events at the single-molecule level.

Using surface plasmon coupling, nanometer-scale interactions below the diffraction limit have been observed. The colocalization of individual integrin surface receptors on a cell membrane was visualized with sub-diffraction resolution using plasmon coupling between pairs of gold nanocrystals in two-dimensional human cervical carcinoma cell culture models.²⁵ The cell adhesion molecule fibronectin was first bound to integrin surface receptors. Single gold nanocrystals, functionalized with

anti-fibronectin, were then bound to the receptors by formation of fibronectin-integrin complexes (Fig. 5A). Lateral movement of individual receptors was then tracked over time by intensity analysis of the ratio of the light scattering intensities at 530 nm and 580 nm. Individual receptors were initially separated. As the moving receptors co-localized, an increase in the ratio of light scattering intensities was seen due to coupling of surface plasmons of the bound nanocrystals (Fig. 5B). Trafficking, clustering, and dimerization of other receptors, such as epidermal growth factor receptors, have also been imaged with sub-diffraction resolution using plasmon coupling.^{27,28,53,54}

Improved temporal resolution of plasmon rulers enables the ability to visualize activity in real time and resolve intermediate dynamics that otherwise would be very difficult to observe using conventional bulk methods with lower temporal resolution. Using plasmon rulers, an intermediate step in enzyme catalysis was captured recently at the single-molecule level.²⁴ Plasmon rulers consisted of a gold nanocrystal dimer linked with DNA containing a single restriction site for the restriction enzyme EcoRV (Fig. 6A). In order to capture enzymatic dynamics on the order of micro- to milli-seconds, changes in plasmon coupling were imaged by intensity analysis rather than spectral analysis. The scattering cross-section of a nanocrystal dimer depends on its interparticle distance. When the restriction enzyme cut the DNA, the nanocrystals separated, resulting in a decrease in the light scattering intensity. Using continuous imaging of single-particle trajectories, an intermediate step was captured where the enzyme, upon binding, momentarily bent the DNA. The bending of the DNA caused the two nanocrystals to become closer, resulting in a decrease in the interparticle distance and therefore an increase in the light scattering intensity (Fig. 6B). The enzyme then cut the DNA and a decrease in the light scattering intensity was seen. The observation of these intermediate dynamics is made possible because of the high temporal resolution of plasmon rulers. In addition to nuclease activity, protease activity has similarly been imaged (Fig. 6C) using peptide-linked nanocrystals.²⁶ As compared with fluorophore-based imaging methods, plasmon rulers do not suffer from photobleaching, and are capable of long-term and continuous

imaging as demonstrated by long-term imaging of caspase protease activity in two-dimensional cell culture models.²⁶ We expect that the improved temporal resolution of plasmon rulers should allow for measurement of intermediate dynamics in activity patterns (Fig. 3C).

In conclusion, plasmon rulers bring significant improvements in spatial and temporal resolution and should enable measurement of more quantitative activity patterns. Complex three-dimensional assemblies are being developed to provide conformational information as well as distance dependence.⁵⁵ Plasmon rulers are currently being developed for quantitative measurement of protease activity during tissue morphogenesis in three-dimensional culture models and in vivo. Global modulation with protease activators/inhibitors or local modulation by optical gene silencing⁵⁵⁻⁵⁸ of proteases can be also utilized to systematically modulate spatiotemporal activity patterns. We expect these models to lead not only to an improved quantitative description of tissue morphogenesis but possibly also to advance therapeutic strategies for the repair of diseased or damaged tissues.

Disclosure of Potential Conflicts of Interest

No potential conflicts of interest were disclosed.

Acknowledgments

The authors thank Younggeun Park, William Curt Hines, Vivian Ferry, Jessica Smith, Hidetoshi Mori, Joni Mott, Irene Kuhn, and Richard Schwarz for helpful discussions and critical reading of the manuscript. SEL was supported by the NIH Ruth L. Kirschstein National Research Service Award (F32 EB013972). The work from APA's laboratory was supported by NIH ARRA Plasmon Rulers (NOT-OD-09-056). The work from MJB's laboratory was supported by grants from the US Department of Energy, Office of Biological and Environmental Research and Low Dose Scientific Focus Area (DE-AC02-05CH1123); by National Cancer Institute (R37CA064786, R01CA057621, R01CA140663, U54CA112970, U01CA143233 and U54CA143836—Bay Area Physical Sciences—Oncology Center, University of California, Berkeley, California); and by US Department of Defense (W81XWH0810736).

References

- Lubarsky B, Krasnow MA. Tube morphogenesis: making and shaping biological tubes. *Cell* 2003; 112:19-28; PMID:12526790; [http://dx.doi.org/10.1016/S0092-8674\(02\)01283-7](http://dx.doi.org/10.1016/S0092-8674(02)01283-7)
- Nelson CM, Bissell MJ. Of extracellular matrix, scaffolds, and signaling: tissue architecture regulates development, homeostasis, and cancer. *Annu Rev Cell Dev Biol* 2006; 22:287-309; PMID:16824016; <http://dx.doi.org/10.1146/annurev.cellbio.22.010305.104315>
- Patel VN, Rebutini IT, Hoffman MP. Salivary gland branching morphogenesis. *Differentiation* 2006; 74:349-64; PMID:16916374; <http://dx.doi.org/10.1111/j.1432-0436.2006.00088.x>
- Yamada KM, Cukierman E. Modeling tissue morphogenesis and cancer in 3D. *Cell* 2007; 130:601-10; PMID:17719539; <http://dx.doi.org/10.1016/j.cell.2007.08.006>
- Lu P, Werb Z. Patterning mechanisms of branched organs. *Science* 2008; 322:1506-9; PMID:19056977; <http://dx.doi.org/10.1126/science.1162783>
- Simian M, Hirai Y, Navre M, Werb Z, Lochter A, Bissell MJ. The interplay of matrix metalloproteinases, morphogens and growth factors is necessary for branching of mammary epithelial cells. *Development* 2001; 128:3117-31; PMID:11688561
- Sympton CJ, Talhouk RS, Bissell MJ, Werb Z. The Role of Metalloproteinases and Their Inhibitors in Regulating Mammary Epithelial Morphology and Function In vivo. *Perspect Drug Discov Des* 1994; 2:401-11; <http://dx.doi.org/10.1007/BF02172033>
- Lü J, Qian J, Keppler D, Cardoso WV, Catespin H. Catespin H is an Fgf10 target involved in Bmp4 degradation during lung branching morphogenesis. *J Biol Chem* 2007; 282:22176-84; PMID:17500053; <http://dx.doi.org/10.1074/jbc.M700063200>
- Moore KA, Polte T, Huang S, Shi B, Alsberg E, Sunday ME, et al. Control of basement membrane remodeling and epithelial branching morphogenesis in embryonic lung by Rho and cytoskeletal tension. *Dev Dyn* 2005; 232:268-81; PMID:15614768; <http://dx.doi.org/10.1002/dvdy.20237>
- Doucet A, Overall CM. Protease proteomics: revealing protease in vivo functions using systems biology approaches. *Mol Aspects Med* 2008; 29:339-58; PMID:18571712; <http://dx.doi.org/10.1016/j.mam.2008.04.003>
- Mason SD, Joyce JA. Proteolytic networks in cancer. *Trends Cell Biol* 2011; 21:228-37; PMID:21232958; <http://dx.doi.org/10.1016/j.tcb.2010.12.002>
- Mott JD, Werb Z. Regulation of matrix biology by matrix metalloproteinases. *Curr Opin Cell Biol* 2004; 16:558-64; PMID:15363807; <http://dx.doi.org/10.1016/j.ccb.2004.07.010>
- Sameni M, Dosesu J, Sloane BF. Imaging proteolysis by living human glioma cells. *Biol Chem* 2001; 382:785-8; PMID:11517931; <http://dx.doi.org/10.1515/BC.2001.094>
- Sabeh F, Shimizu-Hirota R, Weiss SJ. Protease-dependent versus -independent cancer cell invasion programs: three-dimensional amoeboid movement revisited. *J Cell Biol* 2009; 185:11-9; PMID:19332889; <http://dx.doi.org/10.1083/jcb.200807195>

15. Sameni M, Cavallo-Medved D, Dosescu J, Jedeszko C, Moin K, Mullins SR, et al. Imaging and quantifying the dynamics of tumor-associated proteolysis. *Clin Exp Metastasis* 2009; 26:299-309; PMID:19082919; <http://dx.doi.org/10.1007/s10585-008-9218-7>
16. Wolf K, Wu YI, Liu Y, Geiger J, Tam E, Overall C, et al. Multi-step pericellular proteolysis controls the transition from individual to collective cancer cell invasion. *Nat Cell Biol* 2007; 9:893-904; PMID:17618273; <http://dx.doi.org/10.1038/ncb1616>
17. Wolf K, Friedl P. Mapping proteolytic cancer cell-extracellular matrix interfaces. *Clin Exp Metastasis* 2009; 26:289-98; PMID:18600304; <http://dx.doi.org/10.1007/s10585-008-9190-2>
18. Blum G, Mullins SR, Keren K, Fonovic M, Jedeszko C, Rice MJ, et al. Dynamic imaging of protease activity with fluorescently quenched activity-based probes. *Nat Chem Biol* 2005; 1:203-9; PMID:16408036; <http://dx.doi.org/10.1038/nchembio728>
19. Barcellos-Hoff MH, Aggeler J, Ram TG, Bissell MJ. Functional differentiation and alveolar morphogenesis of primary mammary cultures on reconstituted basement membrane. *Development* 1989; 105:223-35; PMID:2806122
20. Petersen OW, Rønnov-Jessen L, Howlett AR, Bissell MJ. Interaction with basement membrane serves to rapidly distinguish growth and differentiation pattern of normal and malignant human breast epithelial cells. *Proc Natl Acad Sci U S A* 1992; 89:9064-8; PMID:1384042; <http://dx.doi.org/10.1073/pnas.89.19.9064>
21. Bissell MJ, Hines WC. Why don't we get more cancer? A proposed role of the microenvironment in restraining cancer progression. *Nat Med* 2011; 17:320-9; PMID:21383745; <http://dx.doi.org/10.1038/nm.2328>
22. Packard BZ, Artym V, Komoriya A, Yamada KM. Direct Visualization of Protease Activity on Cells Migrating in Three-dimensions. *Matrix Biol* 2009; 29:3-10; PMID:19765656; <http://dx.doi.org/10.1016/j.matbio.2008.10.001>
23. Sönnichsen C, Reinhard BM, Liphardt J, Alivisatos AP. A molecular ruler based on plasmon coupling of single gold and silver nanoparticles. *Nat Biotechnol* 2005; 23:741-5; PMID:15908940; <http://dx.doi.org/10.1038/nbt1100>
24. Reinhard BM, Sheikholslami S, Mastroianni A, Alivisatos AP, Liphardt J. Use of plasmon coupling to reveal the dynamics of DNA bending and cleavage by single EcoRV restriction enzymes. *Proc Natl Acad Sci U S A* 2007; 104:2667-72; PMID:17307879; <http://dx.doi.org/10.1073/pnas.0607826104>
25. Rong G, Wang H, Skewis LR, Reinhard BM. Resolving sub-diffraction limit encounters in nanoparticle tracking using live cell plasmon coupling microscopy. *Nano Lett* 2008; 8:3386-93; PMID:18788826; <http://dx.doi.org/10.1021/nl802058q>
26. Jun YW, Sheikholslami S, Hostetter DR, Tajon C, Craik CS, Alivisatos AP. Continuous imaging of plasmon rulers in live cells reveals early-stage caspase-3 activation at the single-molecule level. *Proc Natl Acad Sci U S A* 2009; 106:17735-40; PMID:19805121; <http://dx.doi.org/10.1073/pnas.0907367106>
27. Aaron J, Travis K, Harrison N, Sokolov K. Dynamic imaging of molecular assemblies in live cells based on nanoparticle plasmon resonance coupling. *Nano Lett* 2009; 9:3612-8; PMID:19645464; <http://dx.doi.org/10.1021/nl9018275>
28. Crow MJ, Seekell K, Ostrander JH, Wax A. Monitoring of receptor dimerization using plasmonic coupling of gold nanoparticles. *ACS Nano* 2011; 5:8532-40; PMID:21999459; <http://dx.doi.org/10.1021/nn201451c>
29. Weissleder R, Tung CH, Mahmood U, Bogdanov A Jr. In vivo imaging of tumors with protease-activated near-infrared fluorescent probes. *Nat Biotechnol* 1999; 17:375-8; PMID:10207887; <http://dx.doi.org/10.1038/7933>
30. Bruni-Cardoso A, Vilamaior PS, Taboga SR, Carvalho HF. Localized matrix metalloproteinase (MMP)-2 and MMP-9 activity in the rat ventral prostate during the first week of postnatal development. *Histochem Cell Biol* 2008; 129:805-15; PMID:18320202; <http://dx.doi.org/10.1007/s00418-008-0407-x>
31. Lee SH, Moon JJ, Miller JS, West JL. Poly(ethylene glycol) hydrogels conjugated with a collagenase-sensitive fluorogenic substrate to visualize collagenase activity during three-dimensional cell migration. *Biomaterials* 2007; 28:3163-70; PMID:17395258; <http://dx.doi.org/10.1016/j.biomaterials.2007.03.004>
32. Bremer C, Tung CH, Weissleder R. In vivo molecular target assessment of matrix metalloproteinase inhibition. *Nat Med* 2001; 7:743-8; PMID:11385514; <http://dx.doi.org/10.1038/89126>
33. McIntyre JO, Fingleton B, Wells KS, Piston DW, Lynch CC, Gautam S, et al. Development of a novel fluorogenic proteolytic beacon for in vivo detection and imaging of tumour-associated matrix metalloproteinase-7 activity. *Biochem J* 2004; 377:617-28; PMID:14556651; <http://dx.doi.org/10.1042/BJ20030582>
34. Ouyang M, Lu S, Li XY, Xu J, Seong J, Giepmans BN, et al. Visualization of polarized membrane type 1 matrix metalloproteinase activity in live cells by fluorescence resonance energy transfer imaging. *J Biol Chem* 2008; 283:17740-8; PMID:18441011; <http://dx.doi.org/10.1074/jbc.M709872200>
35. Blum G, von Degenfeld G, Merchant MJ, Blau HM, Bogoy M. Noninvasive optical imaging of cysteine protease activity using fluorescently quenched activity-based probes. *Nat Chem Biol* 2007; 3:668-77; PMID:17828252; <http://dx.doi.org/10.1038/nchembio.2007.26>
36. Chan EWS, Chattopadhyaya S, Panicker RC, Huang X, Yao SQ. Developing Photoactive Affinity Probes for Proteomic Profiling: Hydroxamate-based Probes for Metalloproteinases. *J Am Soc Chem* 2004; 126:14435-46; <http://dx.doi.org/10.1021/ja047044i>
37. Keow JY, Pond ED, Cisar JS, Cravatt BF, Crawford BD. Activity-based Labeling of Matrix Metalloproteinases in Living Vertebrate Embryos. *PLoS ONE* 2012; 7:1-10; <http://dx.doi.org/10.1371/journal.pone.0043434>
38. Saghatelian A, Jessani N, Joseph A, Humphrey M, Cravatt BF. Activity-based probes for the proteomic profiling of metalloproteases. *Proc Natl Acad Sci U S A* 2004; 101:10000-5; PMID:15220480; <http://dx.doi.org/10.1073/pnas.0402784101>
39. Amstad PA, Yu G, Johnson GL, Lee BW, Dhawan S, Phelps DJ. Detection of caspase activation in situ by fluorochrome-labeled caspase inhibitors. *Biotechniques* 2001; 31:608-10, 612, 614 passim; PMID:11570504
40. Bedner E, Smolewski P, Amstad P, Darzynkiewicz Z. Activation of caspases measured in situ by binding of fluorochrome-labeled inhibitors of caspases (FLICA): correlation with DNA fragmentation. *Exp Cell Res* 2000; 259:308-13; PMID:10942603; <http://dx.doi.org/10.1006/excr.2000.4955>
41. Zhu L, Xie J, Swierczewska M, Zhang F, Lin X, Fang X, et al. Dual-functional Receptor-targeted Fluorogenic Probe for In Vivo Imaging of Extracellular Protease Expressions. *Bioconjug Chem* 2011; 22:1011-05; <http://dx.doi.org/10.1021/bc200005w>
42. Chang E, Miller JS, Sun J, Yu WW, Colvin VL, Drezek R, et al. Protease-activated quantum dot probes. *Biochem Biophys Res Commun* 2005; 334:1317-21; PMID:16039606; <http://dx.doi.org/10.1016/j.bbrc.2005.07.028>
43. Peng CW, Liu XL, Chen C, Liu X, Yang XQ, Pang DW, et al. Patterns of cancer invasion revealed by QDs-based quantitative multiplexed imaging of tumor microenvironment. *Biomaterials* 2011; 32:2907-17; PMID:21262536; <http://dx.doi.org/10.1016/j.biomaterials.2010.12.053>
44. Xia Z, Xing Y, So MK, Koh AL, Sinclair R, Rao J. Multiplex detection of protease activity with quantum dot nanosensors prepared by intein-mediated specific bioconjugation. *Anal Chem* 2008; 80:8649-55; PMID:18922019; <http://dx.doi.org/10.1021/ac801562f>
45. Willets KA, Van Duyne RP. Localized surface plasmon resonance spectroscopy and sensing. *Annu Rev Phys Chem* 2007; 58:267-97; PMID:17067281; <http://dx.doi.org/10.1146/annurev.physchem.58.032806.104607>
46. Kelly K, Conorado E, Zhao LL, Schatz GC. The Optical Properties of Metal Nanoparticles: The Influence of Size, Shape, and Dielectric Environment. *J Phys Chem B* 2003; 107:668-77; <http://dx.doi.org/10.1021/jp026731y>
47. Reinhard BM, Siu M, Agarwal H, Alivisatos AP, Liphardt J. Calibration of dynamic molecular rulers based on plasmon coupling between gold nanoparticles. *Nano Lett* 2005; 5:2246-52; PMID:16277462; <http://dx.doi.org/10.1021/nl051592s>
48. Jain PK, Huang W, El-Sayed MA. On the Universal Scaling Behavior of the Distance Decay of Plasmon Coupling in Metal Nanoparticle Pairs: A Plasmon Ruler Equation. *Nano Lett* 2007; 7:2080-8; <http://dx.doi.org/10.1021/nl071008a>
49. Sannomiya T, Hafner C, Voros J. In situ sensing of single binding events by localized surface plasmon resonance. *Nano Lett* 2008; 8:3450-5; PMID:18767880; <http://dx.doi.org/10.1021/nl802317d>
50. Chen JI, Chen Y, Ginger DS. Plasmonic nanoparticle dimers for optical sensing of DNA in complex media. *J Am Chem Soc* 2010; 132:9600-1; PMID:20583833; <http://dx.doi.org/10.1021/ja103240g>
51. Skewis LR, Reinhard BM. Spermidine modulated ribonuclease activity probed by RNA plasmon rulers. *Nano Lett* 2008; 8:214-20; PMID:18052230; <http://dx.doi.org/10.1021/nl0725042>
52. Chen JI, Durkee H, Traxler B, Ginger DS. Optical detection of protein in complex media with plasmonic nanoparticle dimers. *Small* 2011; 7:1993-7; PMID:21671429; <http://dx.doi.org/10.1002/smll.201100617>
53. Wang J, Yu X, Boriskina SV, Reinhard BM. Quantification of differential ErbB1 and ErbB2 cell surface expression and spatial nanoclustering through plasmon coupling. *Nano Lett* 2012; 12:3231-7; PMID:22587495; <http://dx.doi.org/10.1021/nl3012227>
54. Wang H, Rong G, Yan B, Yang L, Reinhard BM. Optical sizing of immunolabel clusters through multispectral plasmon coupling microscopy. *Nano Lett* 2011; 11:498-504; PMID:21247191; <http://dx.doi.org/10.1021/nl103315t>
55. Liu N, Hentschel M, Weiss T, Alivisatos AP, Giessen H. Three-dimensional plasmon rulers. *Science* 2011; 332:1407-10; PMID:21680838; <http://dx.doi.org/10.1126/science.1199958>
56. Lee SE, Liu GL, Kim F, Lee LP. Remote optical switch for localized and selective control of gene interference. *Nano Lett* 2009; 9:562-70; PMID:19128006; <http://dx.doi.org/10.1021/nl802689k>
57. Lee SE, Sasaki DY, Park Y, Xu R, Brennan J, Bissell MJ, et al. Photonic gene circuits by optically addressable siRNA-Au nanoantennas. *ACS Nano* 2012; 6:7770-80; PMID:22827439; <http://dx.doi.org/10.1021/nn301744x>
58. Lee SE, Lee LP. Nanoplasmonic gene regulation. *Curr Opin Chem Biol* 2010; 14:623-33; PMID:20888286; <http://dx.doi.org/10.1016/j.cbpa.2010.08.015>